

## Postponed bifurcations of a ring-laser model with a swept parameter and additive colored noise

R. Mannella, Frank Moss,\* and P. V. E. McClintock

*Department of Physics, University of Lancaster, Lancaster LA1 4YB, England, United Kingdom*

(Received 24 October 1986)

We present measurements of the time evolution of the statistical densities of both amplitude and field intensity obtained from a colored-noise-driven electronic circuit model of a ring laser, as the bifurcation parameter is swept through its critical values. The time-dependent second moments (intensities) were obtained from the densities. In addition, the individual stochastic trajectories were available from which the distribution of bifurcation times was constructed. For short-correlation-time (quasiwhite) noise our results are in quantitative agreement with the recent calculations of Boggi, Colombo, Lugiato, and Mandel [Phys. Rev. A 33, 3635 (1986)]. New results for long noise correlation times are obtained.

### I. INTRODUCTION

Swept and modulated parameter bifurcating systems have become objects of considerable interest,<sup>1-5</sup> stimulated chiefly by applications in optical bistability<sup>6</sup> and the laser transition.<sup>7,8</sup> The general effects of noise at instabilities have been studied extensively.<sup>9</sup> However, more recently, a growing awareness that driven bifurcations do not occur in real physical systems in the absence of noise has developed<sup>10-15</sup> and has been stimulated by a number of experiments.<sup>16-19</sup>

In this paper we study the influence of additive colored noise on the postponed bifurcations of a specific laser model induced by sweeping the bifurcation parameter at a non-negligible velocity. Swept-parameter-induced postponements should be distinguished from purely noise-induced postponements predicted<sup>20</sup> and measured in electronic circuit models<sup>21</sup> some time ago and more recently observed experimentally in transitions to turbulences in liquid crystals<sup>17,18</sup> and in superfluid helium.<sup>22</sup>

The influence of *colored* noise on swept-parameter transitions is extremely difficult to study theoretically, though a first and very approximate attempt together with measurements on a simulator have been reported.<sup>10</sup> Neither is it easy to digitally integrate the appropriate higher-dimensional Fokker-Planck equation for swept-parameter systems subject to time-correlated noise, and no such studies have, to our knowledge, been reported. In such situations, simulations by means of analog electronic circuits<sup>23,24</sup> offer a powerful and convenient tool for testing existing theory<sup>25</sup> and guiding new theoretical studies.<sup>26,27</sup>

We report here measurements made on an analog simulator of the system

$$dx/dt = x[-1 + A(t)/(1+x^2)] + V_n(t), \quad (1a)$$

$$dV_n(t)/dt = (1/\tau)[-V_n + \Gamma(t)], \quad (1b)$$

$$A(t) = A_0 + vt, \quad (1c)$$

where  $A(t)$  is the bifurcation parameter, swept from an initial value  $A_0$  at velocity  $v$ ; and where  $V_n(t)$  is a colored noise with correlation time  $\tau$ . Equation (1b) implies that

the noise is exponentially correlated

$$\langle V_n(t)V_n(s) \rangle = (D/\tau)e^{-|t-s|/\tau} \quad (2)$$

and derives from a white noise source  $\langle \Gamma(t)\Gamma(s) \rangle = (2D)\delta(t-s)$  of intensity  $D$ .

### II. SUMMARY OF THE PREDICTED BEHAVIOR

The model Eq. (1a) has been used by Broggi, Colombo, Lugiato, and Mandel (BCLM) to represent the stochastic dynamics of a tuned, single-mode, homogeneously broadened ring laser in the good cavity limit, and they studied its bifurcation behavior in the white-noise limit of  $V_n(t)$  in a recent publication.<sup>28</sup> BCLM made a deterministic ( $V_n=0$ ) study of Eq. (1) by linearizing it around  $x=0$ . The system bifurcates at  $A(t)=1$  in the static ( $v=0$ ) limit. They found, however, that when  $A$  is swept with  $v>0$  from an initial value  $A_0 < 1$ , the *bifurcation is postponed* to a new value  $A^*$  which is obtained at a new time  $t^*$ , where  $A^* \equiv A(t^*)$ . Remarkably, neither  $A^*$  nor  $t^*$  depend on  $v$ , but instead are given by

$$t^* = 2\bar{t}, \quad (3a)$$

$$A^* - \bar{A} = \bar{A} - A_0, \quad (3b)$$

where the bars indicate the static values. The magnitude of the postponement (beyond the static value) does however depend on  $A_0$ .

The nondeterministic problem  $V_n(t)>0$  was modeled by a one-dimensional white-noise Fokker-Planck equation

$$\partial_T P(x,t) = \partial_x \{ x [ 1 - A(t)/(1+x^2) ] + D \partial_x \} P(x,t), \quad (4)$$

which was numerically integrated for several values of  $A_0$ ,  $D$ , and  $v$  using  $P(x,0) = \delta(x)$  as an initial density. From these densities BCLM obtain the time evolution of the second moment  $\langle x^2 \rangle$ , the laser field intensity, and the distribution of bifurcation times  $W(t)$ , or the equivalent  $W(A)$ . Since the individual stochastic trajectories  $x(t)$  were not available, BCLM obtained  $W(t)$  from an ansatz:

$$P(t) = 2 \int_{x_{th}}^{\infty} P(x,t) dx, \quad (5a)$$

$$W(t) = dP(t)/dt, \quad (5b)$$

which represents the rate of growth of probability accumulated above an arbitrarily defined threshold  $x_{th}$ .

The BCLM results, which are valid only for white noise, can be summarized as follows.

(1) Nonzero noise destroys the singular deterministic behavior predicted by Eqs. (3) by reducing the magnitude of the postponement which can then be restored with a larger sweep velocity.

(2) Increasing noise intensity broadens the distributions  $W(A)$ , which can then be sharpened by reducing the sweep velocity.

Below we describe measurements of  $x(t)$  and  $P(x,t)$  made on an electronic circuit model of Eqs. (1). A preliminary account of our results for quasiwhite noise, which are in quantitative agreement with the BCLM predictions, has been submitted.<sup>29</sup> Here we describe the measurements more completely, and include results for colored noise. As we show below, noise color, even for very large  $\tau$ , has little effect.

### III. THE SIMULATOR

A schematic diagram of the electronic circuit model of Eqs. (1) is shown in Fig. 1. The principle of operation of this simulator is identical with those used in previous works.<sup>25,26</sup> Analog multipliers and dividers are used to generate voltages proportional to each term in Eqs. (1) which are then summed and finally integrated as shown by the appropriate operational symbol on Fig. 1. The noise voltage  $V_n(t)$  was supplied by a generator<sup>30</sup> followed by a linear filter used to set the correlation time.

At the output of the integrator, the voltage is proportional to

$$x(t) = \tau_i^{-1} \int \{x[-1 + A(t')/(1+x^2)] + V_n(t')\} dt', \quad (6)$$

where  $\tau_i$  is the integrator time constant. All time-dependent quantities are scaled by  $\tau_i$ , so that the actual time  $t'$  in Eq. (6) is scaled to the dimensionless time  $t = t'/\tau_i$  which appears in Eqs. (1)–(5). Moreover, the ac-

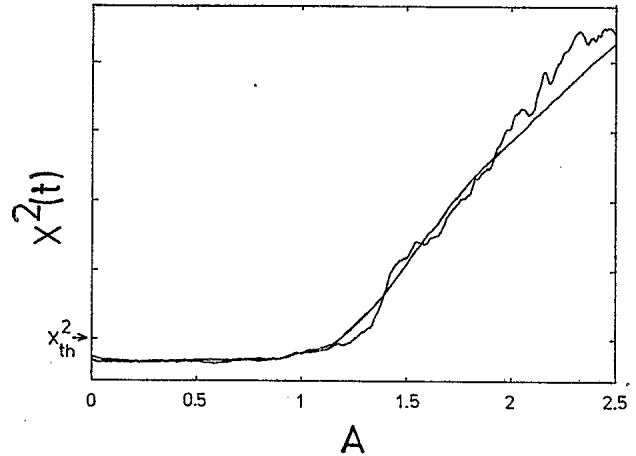


FIG. 2. Example measured trajectories  $x^2(t)$  (arbitrary units). Each trajectory is 4000 digitized points. The noisier trajectory is for  $\tau=0.1$  and the smoother for  $\tau=10$ . The threshold  $x_{th}^2$  is shown.  $A$  is in volts.

tual noise correlation time  $\tau_n$  becomes the dimensionless quantity  $\tau = \tau_n/\tau_i$  which appears in Eqs. (1) and (2). For  $\tau \sim 0.1$  the noise can be described as “quasiwhite,” and we have previously shown that the response of our simulators to such noise is well described by white-noise solutions of one-dimensional Fokker-Planck equations. Throughout the work  $\tau_i = 100 \mu s$  and  $D = 10^{-3} V^2$ . The ranges of the other quantities were  $10 \mu s \leq \tau_n \leq 1000 \mu s$ , and  $10^{-3} \leq v \leq 10^{-1} V$ , where  $v$  is a “dimensionless” velocity, defined by Eq. (1c) and  $t = t'/\tau_i$ , but actually measured in volts.

### IV. CIRCUIT OPERATION AND MEASUREMENTS

As shown on Fig. 1, a triangular wave  $A(t)$  was applied to the circuit. The peak-to-peak amplitude was always 2 V, and the starting value  $A_0$  was normally 0.5 V, but could be adjusted. The period of the triangular waves was adjusted, in accord with the time scaling discussed above, to give the desired value of sweep velocity  $v$  defined in Eq.

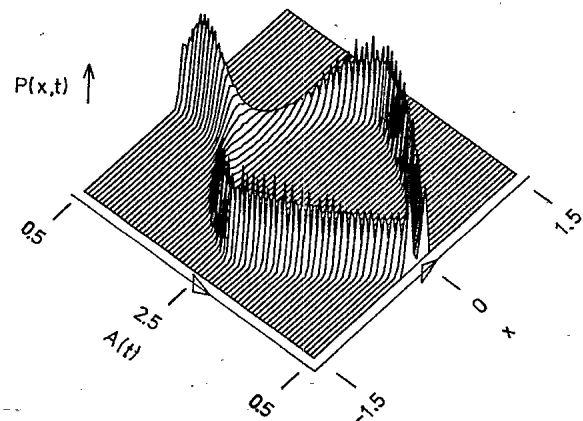


FIG. 3. The time evolving density  $P(x,t)$ . The time axis has been converted to  $A$  in volts with Eq. (1c).  $A(t)$  is swept in the direction of the arrow from 0.5 to +2.5 volts and back to 0.5. For this example,  $D = 10^{-3} V^2$ ,  $v = 10^{-1} V$ , and  $\tau = 0.1$ .

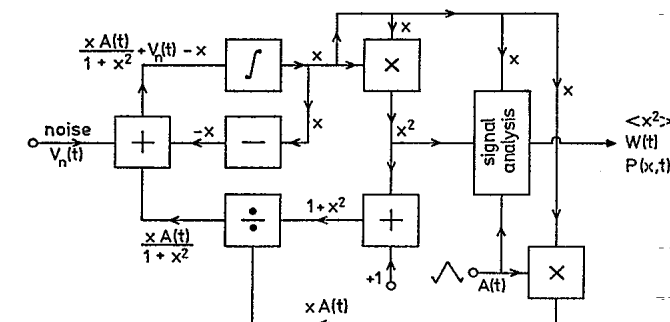


FIG. 1. Schematic diagram of the analog electronic circuit model of Eqs. (1). The multipliers and the divider are Analog Devices Inc. type AD534. The summing and integrating circuits are straightforward operational amplifier designs.

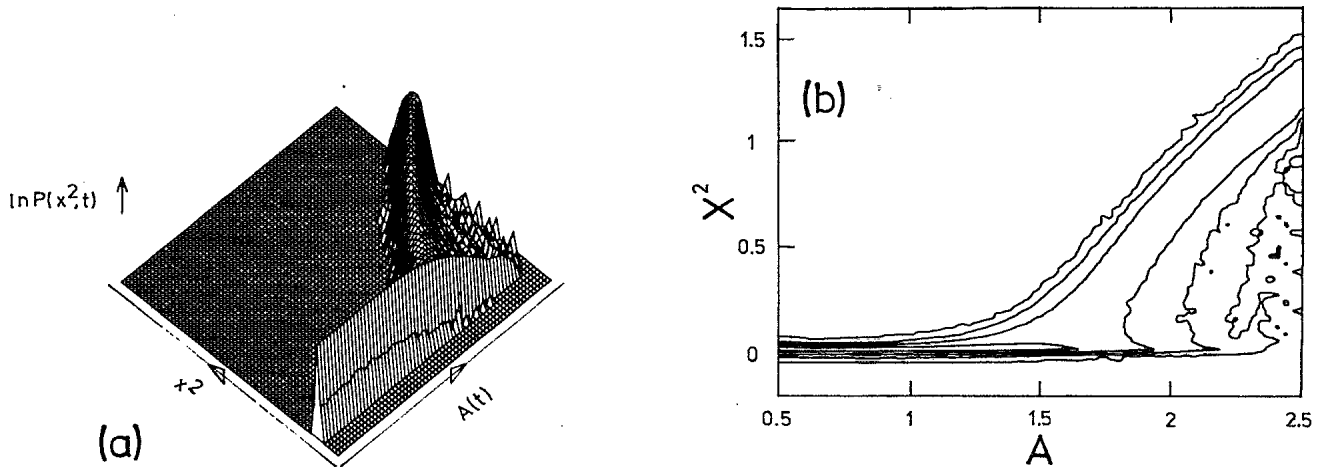


FIG. 4. The time evolving density  $P(x^2, A)$  for  $v=10^{-1}$  V (high sweep speed) and  $\tau=0.1$  (quasiwhite noise). (a) A three-dimensional plot, and (b) a contour plot, where four contours of constant probability [cuts through  $P(x^2, A)$  by planes parallel to the  $x^2, A$  plane] are shown at relative probability altitudes 3, 20, 148, and 1096.  $x^2$  is in  $V^2$  and  $A$  is in V.

(1c). In operation a large number (usually 5000) of stochastic trajectories  $x(t)$  and  $x^2(t)$  were digitized and processed by the signal analysis system (a Nicolet LAB80). Two such example trajectories are shown in Fig. 2 for two correlation times  $\tau=0.1$  and 10, along with the arbitrarily defined threshold  $x_{th}^2$ , to be discussed later. For all the results reported here, the noise intensity was held constant at  $D=10^{-3} V^2$ .

The trajectories  $x(t)$  (not shown) were also measured. It should be noted that at bifurcation the trajectory  $x(t)$  will select and approach the vicinity of either the positive or the negative branch of stable deterministic steady states of Eq. (1a); that is,  $x(t)$  undergoes a pitchfork bifurcation

$$x_{\pm} = \pm\sqrt{A-1}, \quad A > 1. \quad (7)$$

This selection process, which for  $V_n > 0$  is statistical, has been previously discussed for a different system.<sup>10</sup>

It is worth noting that in contrast to the numerical solutions of the Fokker-Planck equation, our system yields the trajectories  $x(t)$  and  $x^2(t)$  immediately as the

measured physical quantities. As discussed below, this allows us to obtain the distribution of bifurcation times  $W(t)$ , in a direct way thereby providing a test of the BCLM result.

From many samples of the measured  $x(t)$ , the time-evolving density  $P(x, t)$  was constructed. An example is shown in Fig. 3 for quasiwhite noise  $\tau=0.1$ . The time axis has been converted to  $A(t)$  using Eq. (1c). The sweep commences on the left at  $A_0=0.5$  V, proceeds in the direction of the arrow to  $A_{max}=2.5$  V, then returns to  $A=0.5$  V on the right. Thus the forward sweep bifurcation is visible on the left and the reverse sweep collapse to the  $x \sim 0$  state on the right. Considerable hysteresis, also noted by BCLM, is evident with the forward sweep transition to bimodality (bifurcation) considerably delayed, and the reverse sweep collapse somewhat prolonged.

Of greater interest here are  $P(x^2, t)$ , which in our system were obtained by analysis of the trajectories  $x^2(t)$ . Two examples, both for high sweep velocity  $v=10^{-1}$  V, are shown in Figs. 4 and 5 for  $\tau=0.1$  and 10, respectively. Examples for low sweep velocity  $v=10^{-3}$  V are shown

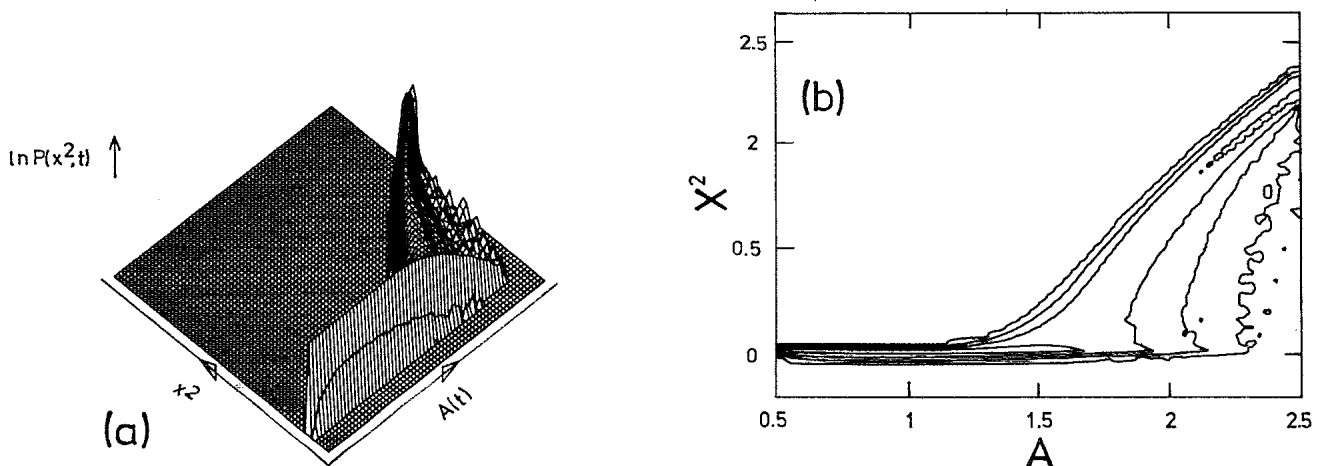


FIG. 5. The time evolving density  $P(x^2, A)$  for  $v=10^{-1}$  V (high sweep speed) and  $\tau=10$  (very colored noise); (a) a three-dimensional plot, and (b) a contour plot, with contour cuts at the same altitudes as in Fig. 4(b).  $x^2$  is in  $V^2$  and  $A$  is in V.

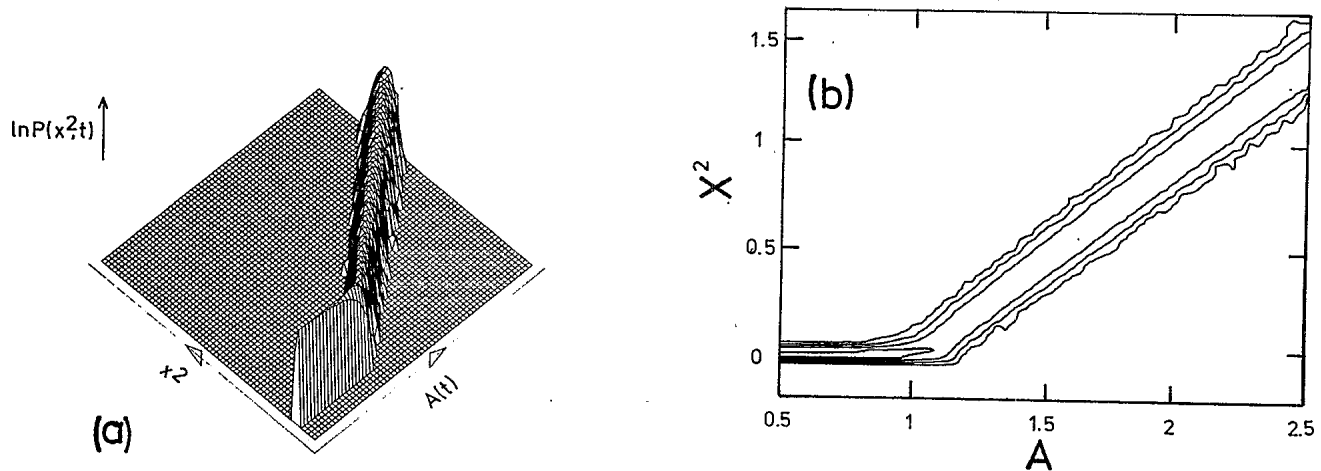


FIG. 6.  $P(x^2, A)$  for  $v=10^{-3}$  V (low sweep speed) and  $\tau=0.1$  (quasiwhite noise); (a) a three-dimensional plot, and (b) a contour plot with contours cut at the same altitudes as Figs. 4(b) and 5(b).  $x^2$  is in  $V^2$  and  $A$  is in V.

also for quasiwhite and very colored noise in Figs. 6 and 7.

It is very obvious from these results that noise color has no appreciable effect on the statistical properties of the bifurcation process at high velocity. A careful comparison of Figs. 4(b) and 5(b) (high velocity) indicates that the leading edges of the contours (left-hand edges) are slightly postponed for large  $\tau$ , while the trailing edges are virtually identical. Figure 6(b) and 7(b) (low velocity) show the postponement plus a discernible sharpening of the densities. In order to form a quantitative comparison, however, it is necessary to obtain the second moments  $\langle x^2 \rangle$  as shown below. The sweep velocity, as noted already,<sup>29</sup> has a large effect by inducing postponements of the bifurcations and by broadening (at large velocity) the densities.

The time evolution of the second moments obtained from densities similar to those discussed above are shown in Figs. 8 and 9, where the results for quasiwhite noise are

shown by the squares and for very colored noise by the diamonds. Figure 8(a) shows a bifurcation at low sweep velocity and Fig. 8(b) at high velocity. The BCLM results are shown by the solid lines, which agree quite well with our measurements for quasiwhite noise. The slight postponement evident at high velocity for colored noise can be observed by comparing squares and diamonds in Fig. 8(b).

In Fig. 9, we show the results of a search for any possible dependence of the bifurcation on  $A_0$ , the initial value of the sweep. BCLM point out that while the deterministic theory predicts such a dependence, as shown by Eq. (3b), white noise should destroy the dependence. They, however, speculate that for colored noise of long correlation times, the  $A_0$  dependence might be restored. We do not observe this, even for  $\tau=10$  as Fig. 9 shows. In fact, we observe only a weak  $A_0$  dependence with zero external noise. Evidently even the very small ( $\sim 0.1$  mV) internal noise destroys the singular deterministic state.

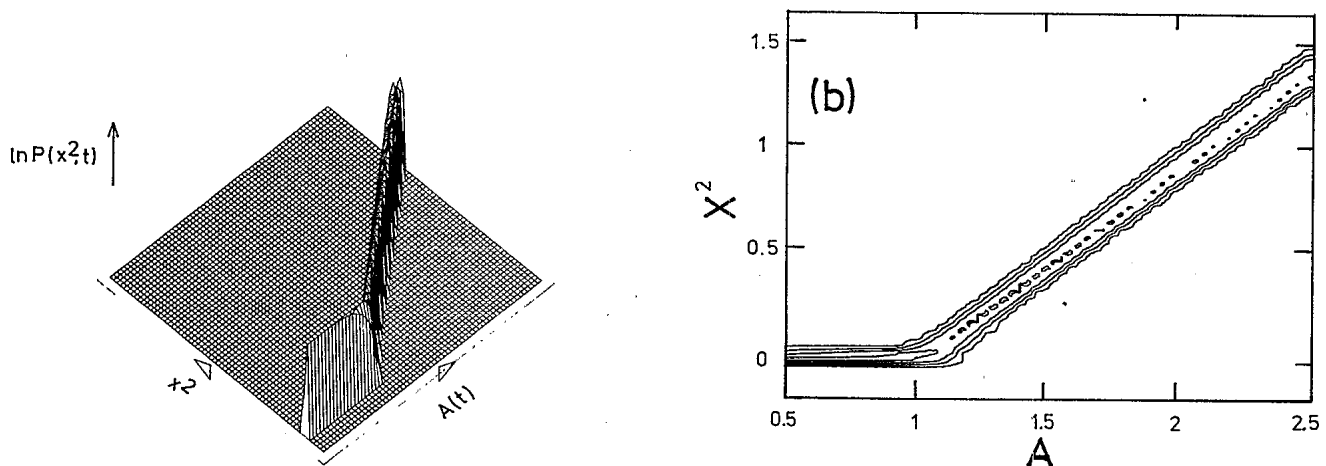


FIG. 7.  $P(x^2, A)$  for  $v=10^{-3}$  V (low sweep speed) and  $\tau=10$  (very colored noise); (a) a three-dimensional plot, and (b) a contour plot with contours cut at the same altitudes as all previous cuts.  $x^2$  is in  $V^2$  and  $A$  is in V.

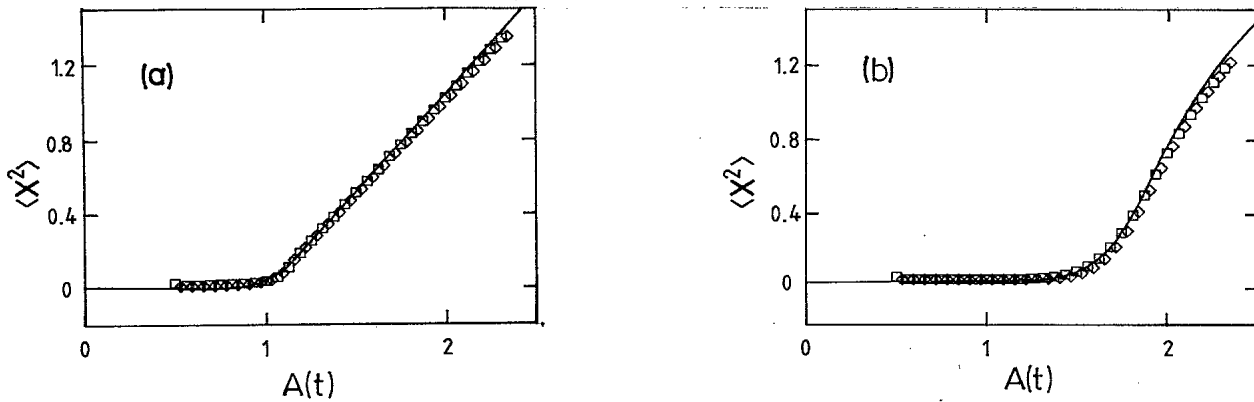


FIG. 8. The time evolution of the second moment for  $\tau=0.1$  (squares) and 10 (diamonds); (a) with  $v=10^{-3}$  V, and (b) with  $v=10^{-1}$  V.  $\langle x^2 \rangle$  is in  $V^2$  and  $A$  is in V. The smooth curves are the results of numerical solutions of Eq. (4) from Ref. 28 BCLM.

### V. THE DISTRIBUTION OF BIFURCATION TIMES

As Fig. 2 shows, the individual trajectories of the laser intensity are noisy. The precise time at which a bifurcation occurs however one chooses to define it, is necessarily a statistical quantity, and it is of interest to obtain its distribution  $W(t)$ , or the equivalent  $W(A)$ .

In fact, bifurcations of the type described here, represent quite general switching events. Since every real switch necessarily operates in the presence of some noise, no matter how small, it is of great practical interest to characterize noisy switching events in a proper statistical sense.<sup>23</sup> The quantity  $W(t)$  is one such characterization.

We define the bifurcation as having occurred at the precise time (or  $A$  value) at which the trajectory  $x^2(t)$  first crosses a threshold  $x_{th}^2(t)$ ; or, in the language of stochastic theory, the first passage time from  $x^2 \equiv 0$  to  $x^2 = x_{th}^2$ . This definition is to be contrasted with that of BCLM who, not having the trajectories  $x^2(t)$  available, used the definition of Eqs. (5). We have measured  $W(A)$  for  $x_{th}^2 = 0.1$ . The results are shown in Fig. 10(a) quasiwhite noise and for three sweep velocities. Since these data are quite scattered, we have made spline fits as shown in Fig.

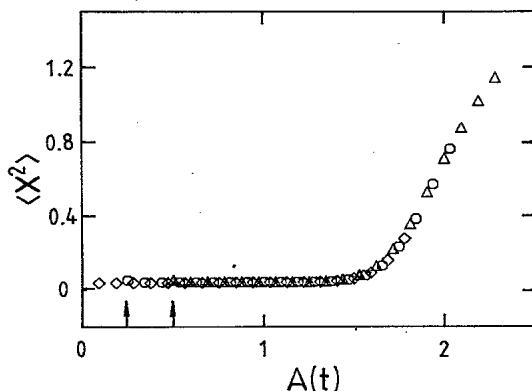


FIG. 9.  $\langle x^2 \rangle$  versus  $A$  for  $\tau=10$  and  $v=10^{-1}$  with initial sweep parameter values,  $A_0=0$  (diamonds); 0.25 V (circles), and 0.5 V (triangles).  $\langle x^2 \rangle$  is in  $V^2$  and  $A$  is in V.

10(b) for both quasiwhite noise, and for colored noise as indicated. [The raw data for the colored noise are not shown in Fig. 10(a).] It is evident that noise color has very little effect on  $W(A)$  apart from a slight sharpening of the distributions and the very small added postponement at the smallest sweep velocity.

We can quantitatively compare our measurements of  $W(A)$  with BCLM (for the quasiwhite noise cases only) by locating the maxima  $A_{max}$  and evaluating the full widths at half maximum  $\Delta$  of the  $W(A)$ . These are shown in Table I.

It is interesting to note that in spite of the different definitions of  $W(A)$ , the two sets of results are in quite good agreement.

### VI. SUMMARY AND CONCLUSIONS

The influence of noise on bifurcations driven by a swept parameter is a problem of general interest for which no satisfactory analytic theory exists. The Fokker-Planck equation of one such system has, however, been numerically integrated for the case of additive white noise. We have compared measurements made on an analog electronic model of that system to the white-noise numerical results. In addition, we have presented the first data on the same system for extremely colored noise. In the latter instance, numerical integration of an appropriate higher-dimensional Fokker-Planck equation would constitute a formidable problem and has not yet been reported. Indeed, it may not now be of any great interest to do this, in view of our conclusion that the color of additive noise has little effect on the bifurcation.

Further, it has been reasoned that the additive noise in

TABLE I. Comparison of the present results for  $W(A)$  with those of BCLM.

$v$	$A_{max}$		$\Delta$	
	Present	BCLM	Present	BCLM
$10^{-3}$	$1.1 \pm 0.1$	1.12	$0.1 \pm 0.05$	0.10
$10^{-2}$	1.2	1.20	0.3	0.14
$10^{-1}$	1.6	1.55	0.4	0.40

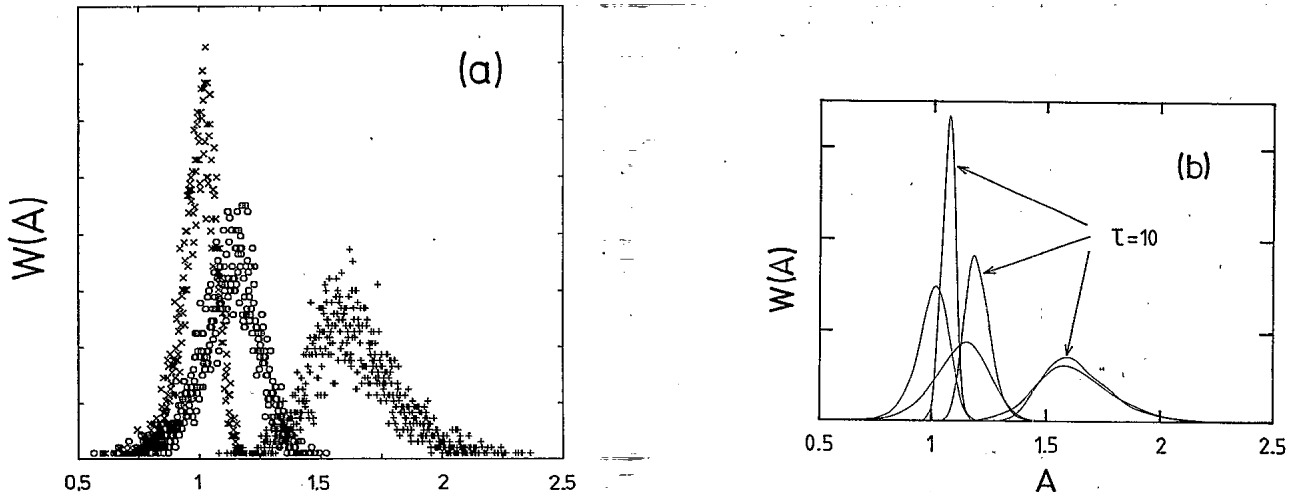


FIG. 10. Distributions of the bifurcation times for  $\nu = 10^{-3}$  V (narrow, large amplitudes),  $10^{-2}$  V, and  $10^{-1}$  V (broad, small amplitude), respectively. (a) The raw data for  $\tau=0.1$ , and (b) spline fits to the raw data for  $\tau=0.1$  and 10. The horizontal axes are in V.

laser models derives from photon emission statistics and is consequently expected to be white. It has very recently been shown in an elegant series of experiments (see the latter entries in Ref. 19) that the pump fluctuations in a dye laser are well represented by colored noise. In laser models, this would appear as multiplicative noise on the pump parameter  $A(t)$ , which it may be of interest to simulate.

Finally, we would emphasize that the measurements presented here have been made on a real physical system, and as such, could with advantage be repeated on an actual laser.

#### ACKNOWLEDGMENTS

We are grateful to Paul Mandel for suggesting these experiments, and to R. Kapral, R. Roy, P. Hanggi, L. Fronzoni, P. Grigolini, E. Arimondo, K. Wiesenfeld, and W. Horsthemke for stimulating discussions. It is a pleasure to thank L. A. Lugiato for an interesting and suggestive correspondence. This work has been supported in part by the British Science and Engineering Research Council, the U.S. Office of Naval Research, Grant No. N00014-85-K-0372, and by North-Atlantic Treaty Organization Grant No. RG.85/0770.

\*Permanent address: Department of Physics, University of Missouri at St. Louis, St. Louis, MO 63121.

<sup>1</sup>P. Mandel and T. Erneux, Phys. Rev. Lett. **53**, 1818 (1984); Phys. Rev. A **30**, 1893 (1984); T. Erneux and P. Mandel, *ibid.* **30**, 1902 (1984).

<sup>2</sup>K. Wiesenfeld and B. McNamara, Phys. Rev. Lett. **55**, 13 (1985); Phys. Rev. A **33**, 629 (1986); P. Bryant and K. Wiesenfeld, *ibid.* **33**, 2525 (1986).

<sup>3</sup>R. Kapral and P. Mandel, Phys. Rev. A **32**, 1076 (1985); T. Erneux and P. Mandel, SIAM J. Appl. Math. **46**, 1 (1986).

<sup>4</sup>M. Lucke and F. Schank, Phys. Rev. Lett. **54**, 1465 (1985).

<sup>5</sup>B. Morris and F. Moss, Phys. Lett. **118A**, 117 (1986).

<sup>6</sup>P. Mandel and T. Erneux, IEEE J. Quantum Electron. **QE-21**, 1352 (1985); R. Valee and C. Delisle, *ibid.* **QE-21**, 1423 (1985).

<sup>7</sup>P. Glorieux and D. Dangoisse, Ref. 6, 1486.

<sup>8</sup>E. Arimondo, C. Gabbanini, E. Menchi, D. Dangoisse, and P. Glorieux, in *Optical Instabilities*, edited by R. W. Boyd, M. G. Raymer, and L. M. Narducci (Cambridge University Press, Cambridge, 1986), p. 277.

<sup>9</sup>For general reviews on the effects of fluctuations on instabilities, see W. Horsthemke and R. Lefever, *Noise Induced Transitions: Theory and Applications in Physics, Chemistry and Biology*, Vol. 15 of *Springer Series in Synergetics* (Springer,

Berlin, 1984); *Fluctuations and Sensitivity in Nonequilibrium Systems*, Vol. I of *Springer Proceedings in Physics*, edited by W. Horsthemke and D. K. Kondepudi (Springer, New York, 1984).

<sup>10</sup>D. K. Kondepudi, F. Moss, and P. V. E. McClintock, Phys. Lett. **112A**, 293 (1985); **114A**, 68 (1986); *Physica (Utrecht)* **21D**, 296 (1986).

<sup>11</sup>G. Broggi and L. A. Lugiato, Phys. Rev. A **29**, 2949 (1984); L. A. Lugiato, A. Colombo, G. Broggi, and R. J. Harowicz, *ibid.* **33**, 4469 (1986).

<sup>12</sup>E. Celarier, S. Frazer, and R. Kapral, Phys. Lett. **94A**, 247 (1983); S. Frazer, E. Celarier, and R. Kapral, J. Stat. Phys. **33**, 341 (1983).

<sup>13</sup>S. J. Linz and M. Lucke, Phys. Rev. A **33**, 2694 (1986).

<sup>14</sup>M. Napionkowski and U. Zaus, J. Stat. Phys. **43**, 349 (1986).

<sup>15</sup>W. Horsthemke, C. R. Doering, R. Lefever, and A. S. Chi, Phys. Rev. A **31**, 1123 (1985).

<sup>16</sup>F. Mitschke, R. Deserno, J. Mlynek, and W. Lange, IEEE J. Quantum Electron. **EQ-21**, 1435 (1985).

<sup>17</sup>H. R. Brand, S. Kai, and S. Wakabayashi, Phys. Rev. Lett. **54**, 555 (1985).

<sup>18</sup>S. Kai, S. Wakabayashi, and M. Imasaki, Phys. Rev. A **33**, 2612 (1986).

<sup>19</sup>R. Roy, R. Short, J. Durnin, and L. Mandel, Phys. Rev. Lett.

- 45, 1486 (1980); S. Zhu, A. W. Yu, and R. Roy, *Phys. Rev. A* **34**, 4333 (1986); R. F. Fox and R. Roy, *ibid.* **35**, 1838 (1987).
- <sup>20</sup>G. V. Welland and F. Moss, *Phys. Lett.* **89A**, 273 (1982); F. Moss and G. V. Welland, *Phys. Rev. A* **25**, 3389 (1982).
- <sup>21</sup>S. D. Robinson, F. Moss, and P. V. E. McClintock, *J. Phys. A* **18**, L89 (1985).
- <sup>22</sup>J. Tough (private communication).
- <sup>23</sup>F. Moss, in *Proceedings of the Workshop on Chaos in Nonlinear Dynamical Systems*, edited by J. Chandra (SIAM, Philadelphia, 1984), Chap. X.
- <sup>24</sup>L. Fronzoni, in *Advances in Nonlinear Dynamic and Stochastic Processes*, edited by R. Livi and A. Politi (World Scientific, Singapore, 1985), p. 201.
- <sup>25</sup>J. Smythe, F. Moss, and P. V. E. McClintock, *Phys. Rev. Lett.* **51**, 1064 (1983); J. M. Sancho, R. Mannella, P. V. E. McClintock, and F. Moss, *Phys. Rev. A* **32**, 3639 (1985); F. Moss and P. V. E. McClintock, *Z. Phys. B* **61**, 381 (1985); R. Mannella, S. Faetti, P. Grigolini, P. V. E. McClintock, and F. Moss, *J. Phys. A* **19**, L699 (1986).
- <sup>26</sup>P. Hanggi, T. Mroczkowski, F. Moss, and P. V. E. McClintock, *Phys. Rev. A* **32**, 695 (1985); L. Fronzoni, P. Grigolini, P. Hanggi, F. Moss, R. Mannella, and P. V. E. McClintock, *ibid.* **33**, 3320 (1986); F. Moss, P. Hanggi, R. Mannella, and P. V. E. McClintock, *ibid.* **33**, 4459 (1986).
- <sup>27</sup>K. Vogel, H. Risken, W. Schleich, M. James, F. Moss, and P. V. E. McClintock, *Phys. Rev. A* **35**, 463 (1987).
- <sup>28</sup>G. Broggi, A. Colombo, L. A. Lugiato, and P. Mandel, *Phys. Rev. A* **33**, 3635 (1986).
- <sup>29</sup>R. Mannella, P. V. E. McClintock, and F. Moss, *Phys. Lett. A* (to be published).
- <sup>30</sup>Wandel and Golterman model RG1.